



## STRENGTH PROPERTIES AND MICROSTRUCTURAL CHARACTERIZATION OF METAKAOLIN GEOPOLYMER CONCRETE SYNTHESIZED AT AMBIENT TEMPERATURE

C. H. Salihu<sup>1\*</sup>, A. E. Abalaka<sup>2</sup>, R. A. Lafiya-Araga<sup>3</sup>, B. J. Olawuyi<sup>2</sup>, I. Kariim<sup>4</sup>

<sup>1</sup>Department of Building, School of Environmental Sciences, Modibbo Adama University of Technology Yola, Adamawa State, Nigeria.

<sup>2</sup>Department of Building, School of Environmental Technology, Federal University of Technology Minna, Niger State, Nigeria.

<sup>3</sup>Department of Chemistry, School of Physical Sciences, Federal University of Technology Minna, Niger State, Nigeria.

<sup>4</sup>Department of Chemical Engineering, School of Engineering and Engineering Technology, Federal University of Technology Minna, Niger State Nigeria

\*Corresponding author's email address: [changliab@gmail.com](mailto:changliab@gmail.com)

### ARTICLE INFORMATION

Submitted 27 March, 2021  
Revised 21 May, 2021  
Accepted 28 May, 2021

### Keywords:

Kaolin  
Geopolymerization  
ambient temperature  
Silicon/Aluminium ratio  
strength properties

### ABSTRACT

Geopolymer concrete has been gaining extensive attention in recent years due to its numerous advantages over Ordinary Portland cement concrete in terms of reduced carbon footprint, improved mechanical strength, durability as well as chemical resistance. However, production of geopolymer concrete is usually affected by several factors such as the synthesis temperature, nature of the source material and the type of alkaline activator used. For these materials to have wider application within the Nigerian construction industry, there is a need to synthesize the concrete at ambient temperature and to examine the suitability of native Alkali kaolin to produce geopolymer concrete. The study presents the strength and microstructural properties of Metakaolin Geopolymer Concrete synthesized at ambient temperature. Alkali calcined kaolin from Bauchi state Nigeria was used as the main geopolymer precursor with sodium hydroxide and sodium silicate as the alkaline activating agent. The Geopolymer concrete was prepared with Silicon/Aluminium ratio of 2.0 and 2.5 (Geopolymer concrete M1 and M2 respectively) and cured for 3, 7, 14, 28, and 90 days at ambient condition (average temperature of 26°C and average relative humidity of 61 ± 15%). Fourier Transform Infra-Red, X-ray Diffraction, Thermo-Gravimetric Analysis, Scanning Electron Microscopy as well as compressive strength and split tensile strength test were conducted on the Geopolymer concrete at appropriate curing age to examine their microstructure and strength properties. The Fourier Transform Infra-Red revealed that there was an immediate geopolymeric reaction between the metakaolin and the alkali activator. The X-ray Diffraction showed that the raw metakaolin sample and both Geopolymer concrete M1 and M2 were amorphous in nature; while the Geopolymer concrete M2 (Silicon/Aluminium ratio of 2.5) exhibited good dissolution of the kaolinite which resulted in a more compact and stable structure in comparison with Geopolymer concrete M1 (Silicon/Aluminium ratio of 2.0). This was also confirmed by the Scanning Electron Microscopic images of the Geopolymer concretes. The Thermo-Gravimetric Analysis revealed that both Geopolymer concrete M1 and M2 were thermally stable at 300°C and at 800°C, only the organic phase of the geopolymer decomposed. The strength properties (compressive and tensile strength) of Geopolymer concrete M1 and M2 increased with increase in the curing age, and Geopolymer concrete M2 displayed slightly higher strength in all the curing ages as compared with the Geopolymer concrete M1. This implies that the higher the Silicon/Aluminium ratio, the higher the mechanical strength of the geopolymer. Both the Geopolymer concrete samples attained a compressive strength that can be acceptable for structural use as normal strength concrete grade C20/25 as specified in the requirement of BS EN 206-1 2000 at 28 days curing.

© 2021 Faculty of Engineering, University of Maiduguri, Nigeria. All rights reserved.

## **1.0 Introduction**

Concrete has gained universal recognition as the most utilized man-made construction material. Consequently, the global consumption of concrete which is estimated to be about 10 billion tons yearly, is believed to rise exponentially primarily been driven by urbanization, industrialization as well as economic growth and expansion taking place around the world (Thapa and Waldmann, 2018).

Making cement for concrete involves heating pulverized limestone and clay to a temperature reaching 1450°C. They chemically interact to form the cementitious compounds in Portland cement. The limestone or calcium carbonate ( $\text{CaCO}_3$ ) is broken down to carbon dioxide gas and calcium oxide when heated to extreme temperatures (Naqi and Jang, 2019). The calcination of the limestone as well as the use of fossil fuels for the heating process releases carbon dioxide into the atmosphere, contributing to global warming. The emissions by cement manufacturing process contributes about 5-7% to the global carbon dioxide emission, estimating it to one tone of carbon dioxide been released to the atmosphere when one tone of Ordinary Portland cement is manufactured (Das *et al.*, 2018; Andrew, 2018). Also, about 1.5 to 1.8 tons of limestone and 0.4 tons of clay are needed to produce every ton of Portland cement (British Geological Survey, 2005). Therefore, the production of Portland cement is an extremely resource and energy intensive process.

The increased use of cement in concrete causing environmental concerns in terms of emission of carbon dioxide during cement manufacture has brought pressure on the Scientists and Engineers to research on other alternative supplementary materials in order to reduce cement consumption in the construction industry. In that regard, geopolymer cements have been proposed in recent years by researchers (Lateef *et al.*, 2016; Shabarish *et al.*, 2018 and Liang *et al.*, 2016) as a greener and more sustainable alternative to OPC and also to address the environmental problems related to the disposal of industrial waste and by-products while reducing costs. Consequently, geopolymerization became popular and geopolymer binders such as Fly Ash (FA), Granulated Blast Furnace Slag (GBFS), Metakaolin (MK) and Silica Fumes (SF) which are termed alumina-silicate materials were adopted and considered more ecologically friendly alternative to Ordinary Portland Cement as their production does not involve limestone calcinations.

Geopolymer binders or cements are used together with aggregates and an alkaline activating solution through a process called geopolymerization to produce geopolymer concretes. Geopolymer concrete (GPC) have been proven by research (Al-Shathr, 2016; Neupane *et al.* 2018) to have superior advantages than Ordinary Portland Cement concrete. Such advantages include but not limited to high early strength, exceptionally high thermal and chemical stability and improved durability that makes this type of concrete acceptable for construction work.

However, geo-polymerization of alumina-silicate materials is affected by several factors which include the synthesis temperature, actual chemical composition of the source material, its particle size distribution, the type of alkaline activator used and the curing temperature (Lateef *et al.*, 2016).

In recent times, investigations have centred on the mechanical, microstructural and durability properties of geopolymer concrete (Diaz-Loya *et al.* 2011; Bashir *et al.*, 2017; Fernandez-  
Corresponding author's e-mail address: [changliab@gmail.com](mailto:changliab@gmail.com)

Jimenez et al., 2006). On factors that affect the geopolymerization, Barbosa et al. (2000) specified on the nature of source material, that geopolymers made from calcined source materials, such as MK, FA, and GBFS yield higher compressive strength when compared to those synthesized from non-calcined materials, such as kaolin clay. Xu and Van Deventer (2000), carried out a study on 15 different natural alumina-silicate materials and reported that alumina-silicates with increased rate of dissolution after polymerisation attained higher compressive strength. The authors concluded that the chemical composition of the alumina-silicate materials such as the percentage of Calcium Oxide (CaO), Potassium Oxide (K<sub>2</sub>O) as well as the molar ratio of Silicon/Aluminium (Si/Al) in the source material, the type of alkaline activator and the molar ratio of (Si/Al) in the alkaline solution during dissolution had significant effect on the compressive strength of the GPC. According to Khale and Chaudhary (2007) the Si/Al ratio of the source material substantially affected the compressive strength of the resulting geo-polymeric products, which increased almost linearly with the Si/Al ratio of geopolymer precursors. A similar conclusion was also pointed out in the study conducted by He et al. (2011) on MK and Red Mud – FA GPC to evaluate the effect of the source materials on the strength and microstructural properties. Correspondingly, in another study, Najet et al. (2013) found that the Si/Al ratio of geopolymer precursor has a significant effect on the mechanical properties and the microstructure of the resulting geo-polymeric products. The authors suggested that more effort should be made to investigate the effects of compositions of alumina-silicate materials from different origin and geopolymers induced under some reaction conditions such as low temperature synthesis (Rovnanik, (2010).

Some studies (Duxson et al., 2007; Kong et al., 2007) carried out on the geopolymeric synthesis of MK to produce GPC revealed that the chemical composition of MK, synthesis and curing temperature significantly affect the final properties of a geo-polymeric product as well as recommend the need to research on locally available MK to understand the extent of reactivity when influenced by different experimental parameters such as Si/Al and ambient temperature synthesis.

Based on these, Nigeria as a developing country has a competitive advantage in the development of this sustainable construction material, because of the large deposit of kaolin scattered in different part of the country. Therefore, the study focuses on a developing field that utilizes cheap and abundant alumina-silicate materials such as kaolin from Alkalari in Bauchi State, Nigeria to make GPC at ambient temperature aimed at examining the strength and microstructural properties with respect to the curing ages of the GPC. This is to identify what variable works best for the indigenous kaolin at the Nigerian climatic condition.

## **2.0 Materials and Methods**

### **2.1 Kaolin**

The kaolin clay which is off-white in color and in powdered form was purchased from local miners at Pali district of Alkalari Local Government Area, Bauchi State, Nigeria. The kaolin sample was calcined in a laboratory furnace at a temperature of 700°C for 3 hours to form MK. The metakaolin obtained was sieved in a 75µm sieve and its chemical composition was examined by way of X-ray fluorescence, which was done at Nigerian Geological Survey Agency Kaduna, following the method outlined by Usman et al. (2020).

## 2.2 Alkaline Solution

12M of Sodium hydroxide solution and sodium silicate solution containing 30.2% SiO<sub>2</sub>, 22.8% Na<sub>2</sub>O and 47% water of crystallization were used as the alkali activator to induce the geopolymerization process. The alkaline activating solution was prepared 24 hours prior to the mixing of concrete (Kamarudin *et al.*, 2011).

## 2.3 Aggregate

Aggregate mostly provide volume stability to concrete and improves its durability. Aggregate which forms 75-80% of the volume of concrete is classified as fine and coarse aggregate (Neville 2000). Sharp river sand was used as fine aggregate because of its lower silt and clay content which can adversely affect the strength of the concrete. It was prepared at saturated surface dry condition following the procedure as outlined in ASTM C128. While crushed granite was used as the coarse aggregate. The coarse aggregates were kept at saturated surface dry condition by soaking in water for 24 hours and surface drying it with a dry towel until all surfaces were dry before experimentation.

## 2.4 Experimental Procedures

For metakaolin (MK) geopolymer concrete (GPC), a total number of fifty (50) 100 x 100 x 100mm concrete cubes as one of the specified size by ASTM C39/C39M-03 (for compressive strength tests) and thirty (30) 150mm□ x 300mm concrete cylinders as specified by ASTM C496/C496M-17 (for split tensile tests) were casted. The experiment was designed for twenty-five (25) cubes, that is (5 cubes for each curing age) and fifteen (15) cylinders (3 cylinders for each curing age) for each Si/Al ratio GPCM1 (Si/Al: 2.0), GPC M2(Si/Al: 2.5). The ASTM standard stipulated a minimum of three specimens for an average strength value at a particular curing age, hence the selection of five (5) number of specimens for compressive strength test and three number of specimens for tensile strength test at each curing age. The curing ages considered for the study were 3, 7, 14, 28- and 90-days. Tables 1, 2, and 3 gives details of number of cubes cast, material composition, specimen number and ratios adopted for the GPC samples.

**Table 1:** Number of cubes for curing age/Si/Al ratio

Curing Age	No. of cubes for compressive strength test		No of cylinders for tensile strength test	
	GPCM1(Si/Al: 2.0)	GPCM2(Si/Al: 2.5)	GPC M1	GPC M2
3	5	5	3	3
7	5	5	3	3
14	5	5	3	3
28	5	5	3	3
90	5	5	3	3
<b>Total</b>	<b>25</b>	<b>25</b>	<b>15</b>	<b>15</b>

**Table 2:** Volume of materials for Geopolymer concrete

Specimen	Si/Al Ratio	MK (kg)	Fine aggregate (kg)	Coarse aggregate (kg)	NaOH (kg)	Na <sub>2</sub> SiO <sub>3</sub> (kg)	Water (kg)
GPC M1	2.0	1.87	2.52	5.90	0.41	0.53	0.65
GPC M2	2.5	1.87	2.52	5.90	0.26	0.68	0.65

**Table 3:** Ratios of materials for Geopolymer concrete

Specimen	Si/Al	Na <sub>2</sub> SiO <sub>3</sub> /NaOH	SiO <sub>2</sub> /Na <sub>2</sub> O	Concentration of NaOH (Mol/L)	H <sub>2</sub> O/MK
GPC M1	2.0	1.3	2.4	12	0.35
GPC M2	2.5	2.6	2.4	12	0.35

#### 2.4.1 Geopolymer Concrete Production.

For the purpose of this study/research, MK GPC was prepared at Si/Al ratios of 2.0 and 2.5, cured at ambient temperature for 3, 7, 14, 28 and 90 days. The experiment adopted the separate mixing method as reported by Rattanasak and Chindaprasirt (2009). The Alkaline activating solution was prepared 24 hours prior to the time of mixing the concrete. This was done by dissolving 480g of Sodium Hydroxide pellets in one liter of water and allowed to cool down to room temperature. The Sodium silicate solution was weighed based on the Si/Al ratio and added to the sodium hydroxide solution (Usman et al., 2020). Predetermined quantity of dry MK powder for each Si/Al ratio and the alkaline solution (table 2) were poured into the concrete mixer and the precise quantity of water according to the water/cement ratio was also added. These materials were mixed for 20 minutes and the fresh geopolymer matrix was poured into 50mm cubic steel molds which were used to examine the microstructure after geopolymerization. The required measure of fine and coarse aggregates (table 2) was poured into the geopolymer paste and the mixing continued for another 20 minutes. The fresh GPC obtained was then transferred into 100mm cubic steel molds for compressive strength test and 150mm  $\Theta$  x 300mm cylindrical steel molds for tensile strength test. Curing of the geopolymer specimens was done in a laboratory ambient environment for 3, 7, 14, 28 and 90 days. The average temperature of the laboratory as at the time of curing was 26.6°C. The relative humidity was 62% at 3- and 7-days curing, 31% at 14 and 28 days curing and 22% at 90 days curing age. During curing, all specimens were covered with a plastic film to prevent quick drying of the concrete specimens.

#### 2.4.2 Microstructural Characterization of Geopolymer

Fourier Transform Infra-red (FTIR), X- Ray Diffraction (XRD), Thermo-Gravimetric Analysis (TGA) and Scanning Electron Microscopy (SEM), were the key tools used in this study for investigating the composition, microstructure, chemical elements and the thermal properties of the constituent materials used in the experiment and the geopolymer produced.

##### 2.4.2.1 Attenuated Total Reflectance – Fourier Transform Infra-Red (ATR-FTIR)

Fourier Transform-Infrared (FTIR) spectroscopy was used to characterize and identify the geopolymerization by means of transmitting the infra-red radiation directly through the sample. This was done at National Research Institute for Chemical Technology (NARICT) Zaria Kaduna State, Nigeria.

The specimens were ground to powder and small amount of potassium bromide (KBr) was added to each sample and they were placed in a mould. Cold press machine was used to press the mould which contains the geopolymer powder and potassium bromide (KBr) at 6 ton for 3 minutes to form pellets for examination. Shimadzu FTIR 8400s Fourier Infra-Red Spectrometer (U.S.A) was used to evaluate the functional group of the sample. FTIR absorption spectra were

recorded in the range of  $400 - 4000\text{cm}^{-1}$  using a spectral resolution of  $2\text{ cm}^{-1}$ . The spectrum of each sample represents an average of 32 scans (Mousa 2013).

#### **2.4.2.2 X-ray Diffraction (XRD)**

X-ray diffraction on MK and resulting geopolymers was done to give more details about the microstructure and chemical composition of the GPC. Following the procedure reported by Soleimani *et al.* (2012), the GPC specimens were grounded into powder and scanned with  $\text{CuK}\alpha$  radiation having generator voltage of 45 kV and tube current of 40mA. The diffractive patterns of the MK and GPC were gotten at  $1^\circ$  per 3.5 minutes over an interval of  $2\theta = 5^\circ - 80^\circ$  and steps of  $2\theta = 0.02^\circ$ . The procedure was performed at the Nigerian Geological Survey Agency in Kaduna, Nigeria using Empyrean XRD diffractometer by P-Analytical B.V (Netherlands).

#### **2.4.2.3 Thermal Gravimetric Analysis (TGA)**

Thermal Gravimetric Analysis is a method of thermal analysis in which changes in weight of a sample is measured as a function of temperature or time in a controlled atmosphere. TGA was carried out at Step-B Laboratory of Federal University of Technology, Minna using TGA 4000 manufactured by PerkinElmer (Netherlands). 13.836 mg of GPC M1 and 16.367 mg of GPC M2 in powdered form were scanned (heated) from  $50^\circ\text{C}$  to  $900^\circ\text{C}$  at  $10^\circ\text{C}/\text{min}$  in a nitrogen environment at a flow rate of 20 ml/min (Rosas *et al.*, 2014)

#### **2.4.2.4 Scanning Electron Microscopy (SEM)**

Scanning Electron Microscopy (SEM) was carried out at Chemical Engineering Department of Ahmadu Bello University, Zaria on the impact fractured surfaces of the different compositions of the geopolymer. The concrete specimens were cut into thin sections and coated with gold before transferring to the sample holder for imaging using JEOL-6400 Model Scanning Electron Microscope (Kamarudin *et al.*, 2011). The images were captured at 5mm working distance with the accelerating voltage of 15kv. The Emission current was  $10\mu\text{A}$  which was adjusted from time to time.

#### **2.4.2.5.1 Strength Properties of Geopolymer Concrete**

Compressive strength and split tensile strength tests were performed on the GPC to examine their mechanical properties at different Si/Al ratio (2.0 and 2.5) and at different curing ages considered (3, 7, 14, 28 and 90 days). Compressive strength test of the geopolymer specimens was performed according to the specifications of ASTM C39/C39M-03. Specimens for the compressive strength test were crushed using the Compression Testing machine (10KN) MODE\_JYS2000A at the Building Department laboratory, FUT Minna. An average crushing load of 5 specimens was obtained for each of the curing age and the compressive strength ( $\text{N}/\text{mm}^2$ ) was calculated by dividing the maximum crushing load (N) by the area of the concrete cubes ( $\text{mm}^2$ ).

$$\begin{aligned} & \text{Compressive strength of concrete cube} \\ & = \frac{\text{Maximun load applied to the cube specimen}}{\text{Cross sectional area of cube specimen}} \end{aligned}$$

Split tensile strength test was carried out on the GPC sample at the appropriate curing age using the modified form of ASTM C496/C496M-17. The concrete cylinders were crushed using the Universal testing machine UTM3000 (30KN) at the Building department Laboratory, FUT Minna. For better comparison of result and to obtain an average tensile load, 3 samples were tested for each curing age. The tensile strength was found by dividing the maximum crushing load by the cross-sectional area of the cylinder.

$$\text{Tensile strength of concrete} = \frac{\text{Maximum load applied to concrete cylinder}}{\text{Cross-sectional area of the cylinder}} \quad (1)$$

### 3.0 Results and Discussion

#### 3.1 Chemical Composition of Metakaolin

Table 4 present the oxides found in metakaolin, having  $\text{Al}_2\text{O}_3$  and  $\text{SiO}_2$  as the major oxides and traces of other oxides. As seen on the percentages of the major oxides, the metakaolin has Si/Al ratio of 1.65 making it adequate for geopolymerization (Kim, 2012).

**Table 4:** Chemical composition of Metakaolin

Oxides	$\text{Al}_2\text{O}_3$	$\text{SiO}_2$	$\text{SO}_3$	$\text{K}_2\text{O}$	$\text{CaO}$	$\text{TiO}$	$\text{V}_2\text{O}_5$	$\text{Cr}_2\text{O}_3$	$\text{MnO}$	$\text{Fe}_2\text{O}_3$
Mass (%)	34.30	54.70	-	0.771	0.385	3.87	0.17	0.054	0.01	2.02
Oxides	$\text{Ga}_2\text{O}_3$	$\text{ZnO}$	$\text{IrO}_2$	$\text{Re}_2\text{O}_7$	$\text{Eu}_2\text{O}_3$	L.O.I	$\text{NiO}$	$\text{Yb}_2\text{O}_3$	$\text{CuO}$	
Mass (%)	0.041	0.01	0.07	0.13	0.084	3.30	0.006	0.040	0.016	

Source: XRF Result from Nigerian Geological Survey Agency Kaduna

#### 3.2 Sieve Analysis of Fine and Coarse aggregate

The results of the sieve analysis for the fine and coarse aggregate are shown on the grain size distribution curve (Figure 1).

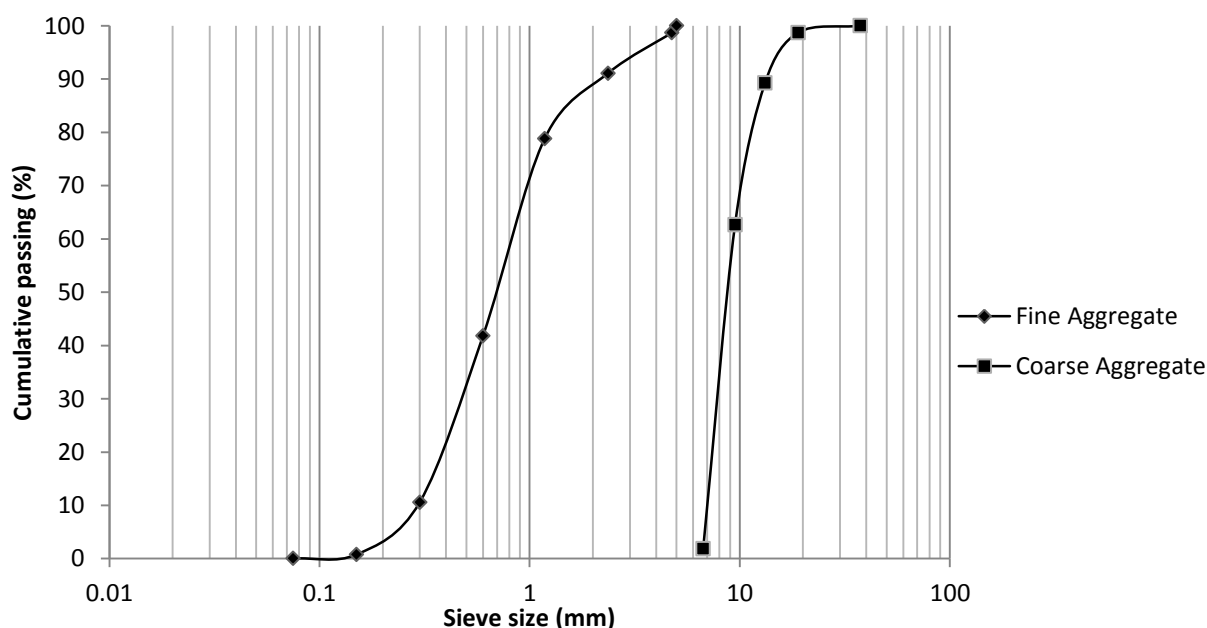


**Figure 1:** Grain size distribution curve of fine and coarse aggregate

Coefficient of Uniformity (Cu) and coefficient of curvature (Cc) of fine aggregate

Coefficient of uniformity (Cu) = 2.96

Coefficient of curvature (Cc) = 0.95

Classification of sand = Uniformly graded or poorly graded since it did not meet the criteria  $C_u \geq 6$  for well graded soil and  $1 < C_c < 3$  for coefficient of curvature

Coefficient of Uniformity ( $C_u$ ) and coefficient of curvature ( $C_c$ ) of coarse aggregate

Coefficient of uniformity ( $C_u$ ) = 1.37

Coefficient of curvature ( $C_c$ ) = 0.95

Classification of coarse aggregate = Uniformly graded or poorly graded since it did not meet the criteria  $C_u \geq 4$  for well graded gravel and  $1 < C_c < 3$  for coefficient of curvature.

The grain distribution curve of fine and coarse aggregate shows that they are both uniformly graded. This means that most of the aggregate particles (both fine and Coarse) are in a very narrow size range or are approximately the same size (Malewar *et al.*, 2017; Pawar *et al.*, 2016). The use of uniformly graded aggregate entrapped more voids within the concrete mass which could increase its permeability and subsequently reduce the mechanical strength. Good compaction of the fresh concrete was done to mitigate the effect of using the uniformly graded aggregate.

### **3.3 Microstructural Properties of GPC**

#### **3.2.1 Fourier Transform Infra-Red of GPC**

Figure 2 and 3 presents the FTIR spectra of MK, GPC M1 and M2 at all the curing ages considered.

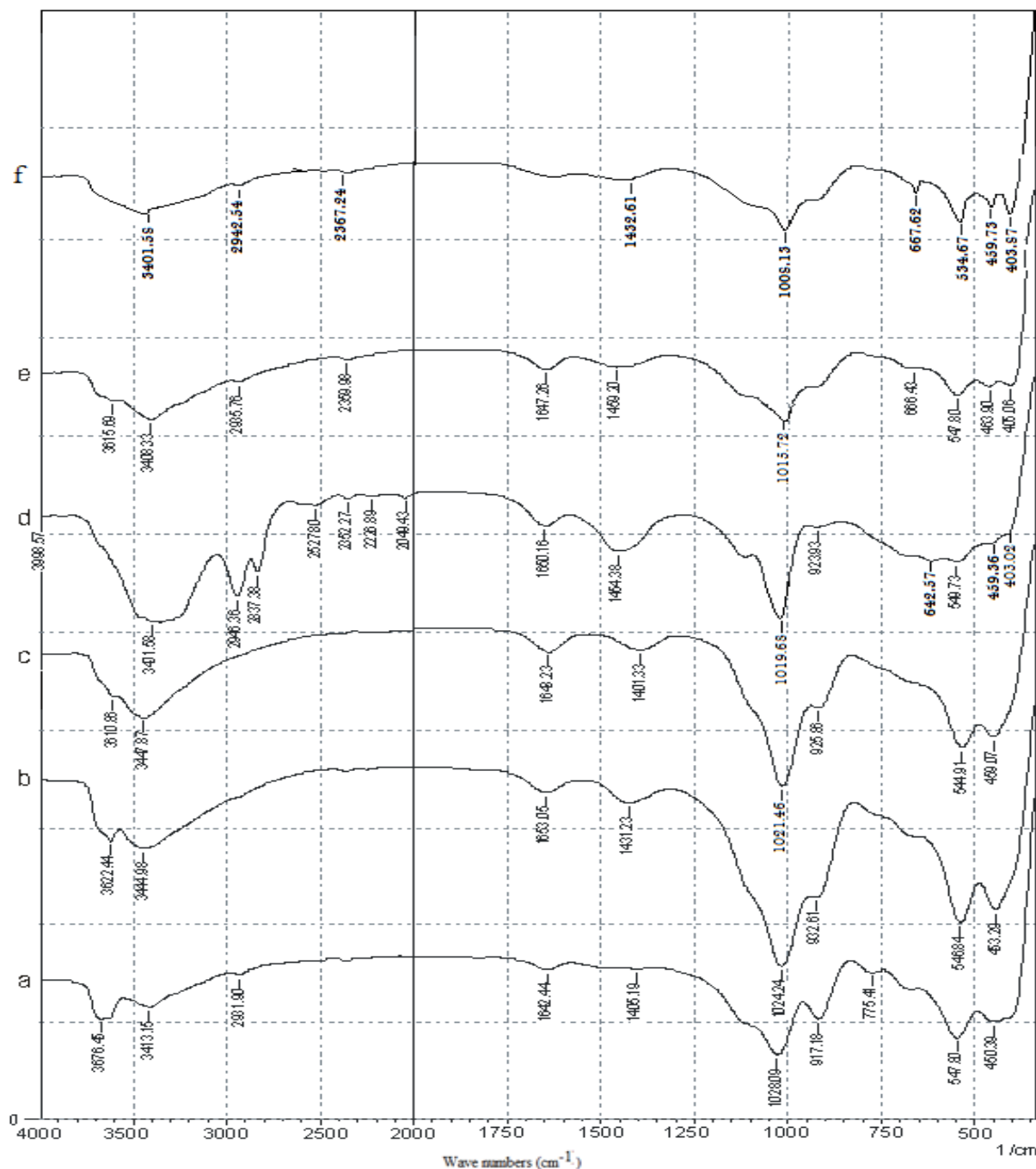


**Figure 2:** FTIR spectra of (a)- MK, GPC M1 at (b)- 3 days, (c)- 7 days (d)- 14 days, (e)- 28 days curing and (f)- 90 days curing ages

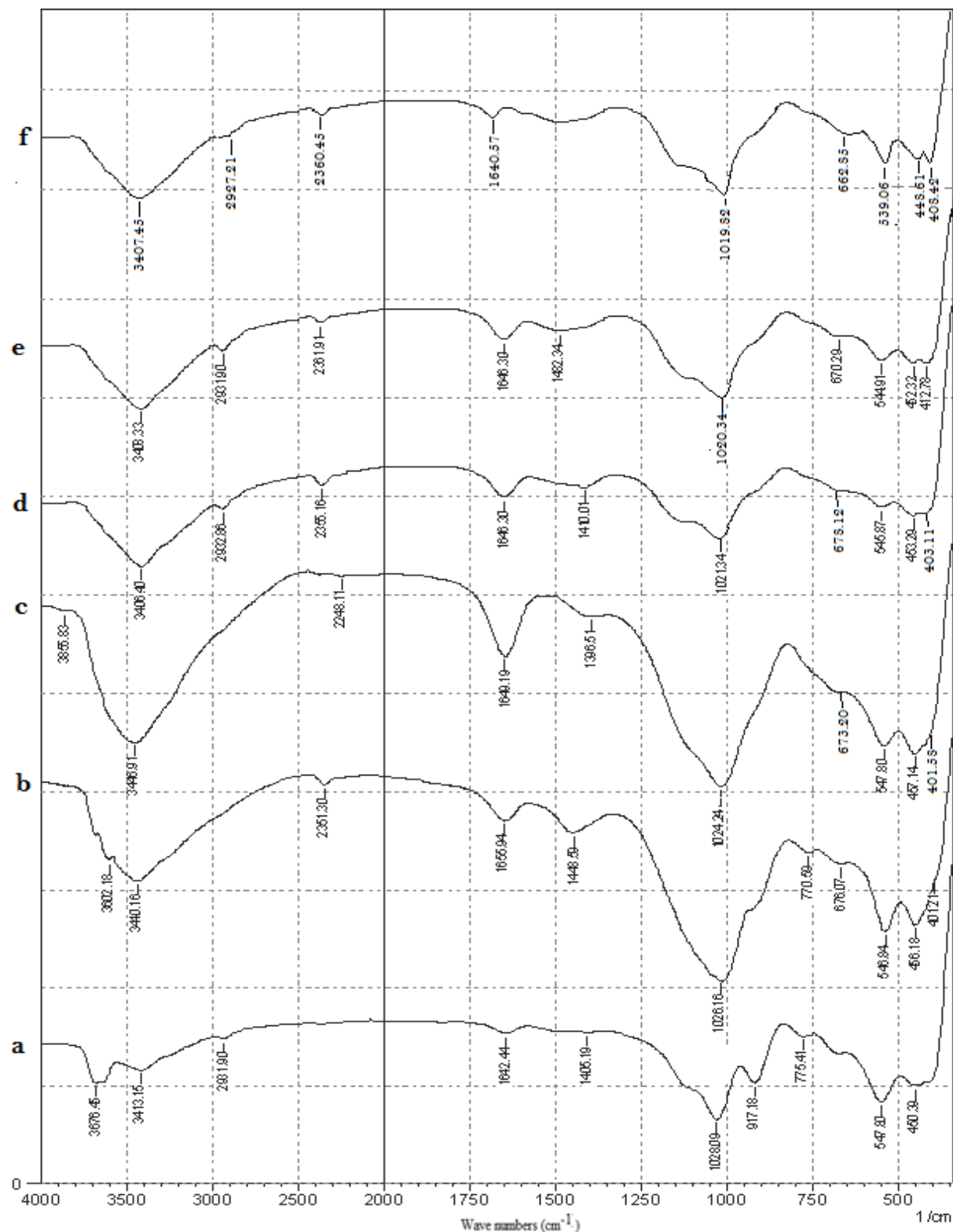


**Figure 3:** FTIR spectral of (a)- MK, GPC M2 at (b)- 3 days (c)- 7 days (d)- 14 days, (e)- 28 days (f)- 90 day curing ages

The FTIR spectrum of kaolin calcined at  $700^{\circ}\text{C}$  for 3 hours is presented in Figure 2a. The spectrum is characterized by series of vibration bands, indicating Si-O bending vibration at about  $450\text{ cm}^{-1}$ , 4-co-ordinate vibration of Al(IV)-O at  $917\text{ cm}^{-1}$  and Si-O-Al vibration at  $775\text{ cm}^{-1}$ . The broad band in the region of  $3413\text{ cm}^{-1}$  and  $1642\text{ cm}^{-1}$  are general characteristic bands

showing O-H and H-O-H groups from weakly bound water molecules and absorbed atmospheric water (Soleiman et al., 2012).

Figure 2 and 3 show the FTIR spectra of GPC M1 and GPC M2 respectively, cured at 3, 7, 14, 28 and 90 days. After the geopolymerization, the following changes were noted:

There was a major disruption of the Al environment as indicated by the reduction of the band at  $775\text{ cm}^{-1}$ , corresponding to Si-O-Al vibration at 3 days and its subsequent disappearance from the 7-days curing age in both GPC M1 and GPC M2. This confirms an immediate reaction between the MK and the alkaline solution.

Evidence of shift was seen in the characteristic band at  $1028\text{ cm}^{-1}$  relating to the Si-O asymmetric stretching towards lower wave numbers after the geopolymerization. The shifts to lower wave numbers became prominent in GPC M1 (Si/Al:2.0) at 14, 28 and 90 days. However, for GPC M2 (Si/Al: 2.5), the shift was seen to have occurred from 3 days and subsequently, 7, 14, 28 and 90 days. Soleimani et al. (2012) suggested that this shift indicates the formation of new structure different from the MK. The authors inferred that the large shift towards lower wave numbers is an evidence of geopolymerization that occurred with the partial replacement of  $\text{SiO}_4$  tetrahedral by  $\text{AlO}_4$  tetrahedral, resulting in a change and reorganization in the local chemical environment of Si-O bond.

The 4-co-ordinate vibration of Al(IV)-O at  $917\text{ cm}^{-1}$  present in the MK sample and GPC M1 was seen to have disappeared as the Si/Al ratio was increased to 2.5 as shown in Figure 3. This is an indication of the displacement of Al in the MK by Si forming Si-O-Si-O-Al bonds, accounting for the increase in the mechanical strength of GPC M2.

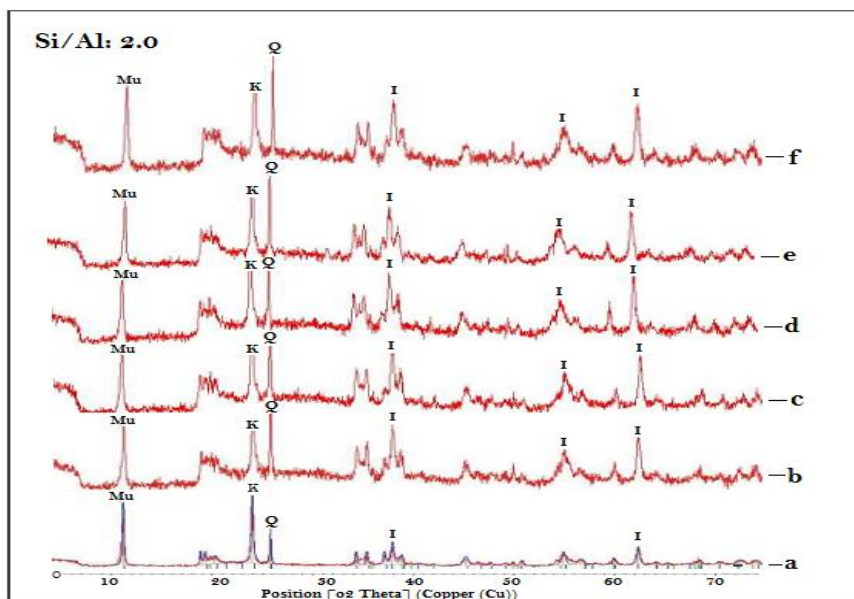
The number of bands in the range of  $400\text{-}600\text{ cm}^{-1}$  in the FTIR spectra of GPC increased considerably for GPC M2 at 3, 7, 14, 28 and 90 days while the increase in the number of bands in that region for GPC M1 was evident from 14 days. This indicates that the geopolymer sample with the higher Si/Al ratio is more suitable for geopolymerization and the rate of strength gain seems to increase with curing age.

The characteristic bands at  $3413\text{ cm}^{-1}$  and  $1642\text{ cm}^{-1}$  corresponding to the presence of absorbed water and weakly bound water molecules (Nasab et al., 2014) was seen to have increased in intensity in the geopolymer samples cured at 3 and 7 days, owing to the presence of additional water that was employed during the casting of the GPC. There was a decrease in the intensities of this bands at later curing ages of 14, 28 and 90 days in both GPC M1 and GPC M2, indicating that the geopolymer samples became drier.

An absorption band at  $1405\text{ cm}^{-1}$  related to  $\text{Na}_2\text{CO}_3$  (Claudio et al., 2013) was present in all the spectra of the geopolymer samples. The existence of this peak could be related to unreacted NaOH, which was carbonated by the  $\text{CO}_2$  in the atmosphere.

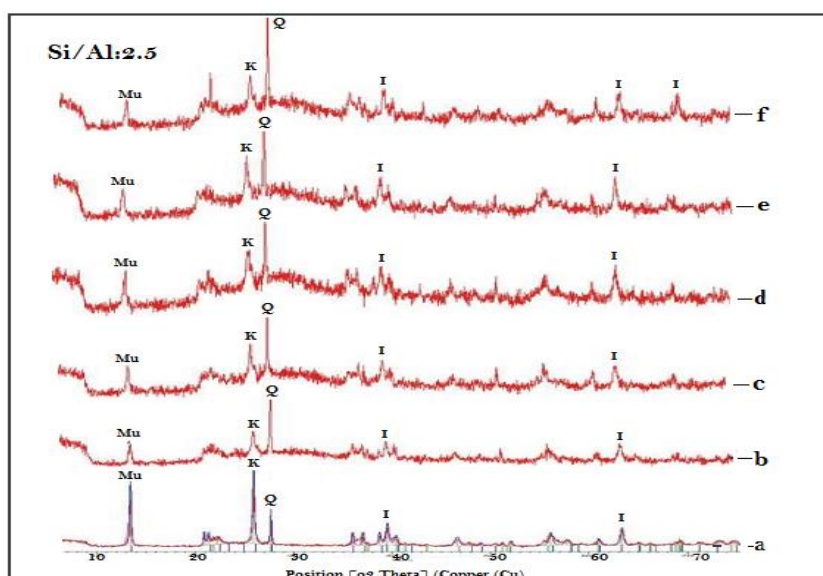
### 3.2.2 X-Ray Diffraction (X-Ray)

Figure 4 and 5 shows the X-ray Diffractive patterns of the MK and the GPC at different curing ages.



K: Kaolinite, Mu: Muscovite, Z: Zeolite, I: Illite, Q: Quartz.

**Figure 4:** X-Ray Diffraction patterns of (a)- MK , GPC M1 at (b) 3 days, (c) 7 days, (d) 14 days, (e) 28 days and (f) 90 days curing ages



K: Kaolinite, Mu: Muscovite, Z: Zeolite, I: Illite, Q: Quartz.

**Figure 5:** X-Ray Diffraction patterns of (a) MK, GPC M2 at (b) 3 days, (c) 7 days, (d) 14 days, (e) 28 days and (f) 90 days curing ages

Amorphous phases such as calcined silica and alumina were identified in the MK by the X-ray diffraction which were indicated by the presence of large halo peaks centered on  $2\theta = 20^\circ - 30^\circ$ . The X-Ray diffraction (XRD) patterns presented sharp peaks at  $2\theta = 12^\circ$ ,  $2\theta = 25^\circ$  and  $2\theta = 27^\circ$ , as seen in Figure 4a, detailing the presence of Muscovite, Kaolinite and Quartz respectively.

The major features of the X-ray diffraction patterns of GPC M1 cured at different ages (Figure 4b, c, d, e and f) are sharp peaks centered at approximately  $12^\circ$  indicating Muscovite,  $25^\circ$  signifying kaolinite,  $27^\circ$  representing Quartz and trace amount of illite at  $35^\circ$ -  $62^\circ$ , which is a characteristic reflection of amorphous geopolymer (Guo et al., 2010). There was incomplete geopolymerization reaction as seen on the diffraction peak revealing the presence of kaolinite which was not properly dissolved by the alkaline activating solution. In the geopolymerisation process, the MK particles are dissolved by the alkali solution (Nasab et al., 2014), indicating that the lower Si/Al ratio (2.0) accounted for the incomplete dissolution of the kaolinite. Crystalline phases in the parent material such as quartz did not take part in the polymerization at the Si/Al: 2.0 as can be seen in the patterns since there was no reduction in the intensities of the peaks after the geopolymerization reaction. This agrees with the current understanding that amorphous phases in raw materials are more reactive and more involved in geopolymerization reactions (Zhang et al., 2010).

For the GPC M2, the X- Ray diffraction patterns at the curing ages of 3, 7, 14, 28 and 90 days (Figures 5b, c, d, e and f) were characterized by sharp peaks at  $2\theta = 12^\circ$ ,  $25^\circ$  and  $27^\circ$ , indicating the presence of Muscovite, Kaolinite and Quartz in the GPC sample respectively as observed earlier in GPC M1. Trace amount of Illite was also detected at  $2\theta = 38^\circ$ -  $62^\circ$ . The peaks relative to Kaolinites decreased as the Si/Al ratio increased to 2.5 which indicate that with higher amount of sodium silicate, most of the kaolinite dissolved and contributed to the geopolymerization. In addition, the intensity of peaks relative to Muscovite and Illite that appeared in the diffractogram of GPC M1 decreased as the Si/Al ratio increased to 2.5. This shows that as the concentration of silicon increases there was further dissolution of Muscovite and Illite present in the MK sample which also contributed in the geopolymerization process, thereby resulting to more orderly and stable phases in their spectra as compared to the one with lower Si/Al ratio.

### 3.2.3 Thermo-Gravimetric Analysis (TGA)

Figures 6 and 7 present the Thermo-Gravimetric Analysis (TGA) and Derivative Thermo-Gravimetric (DTG) curves of the GPC M1 and GPC M2. Table 5 further summarise the result of TGA of the GPC samples.

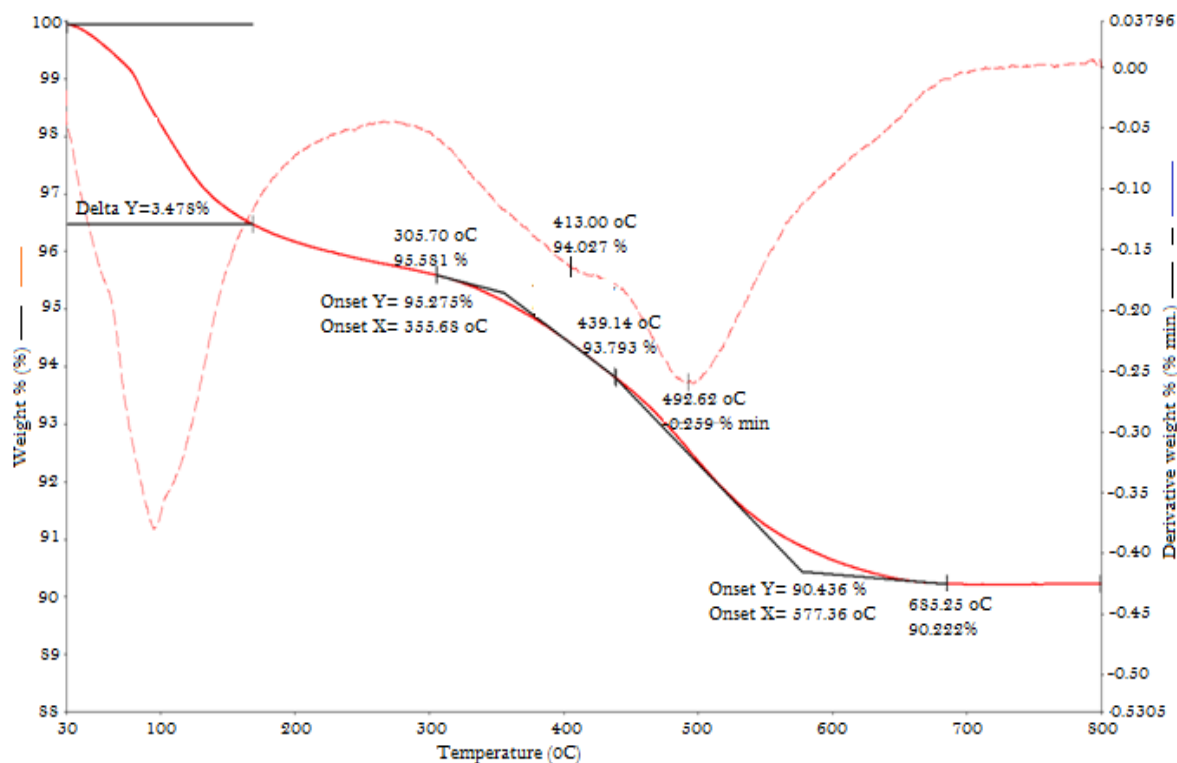


**Figure 6:** Thermogravimetric and Derivative Thermogravimetric analysis of GPC MI (Si/Al: 2.0)

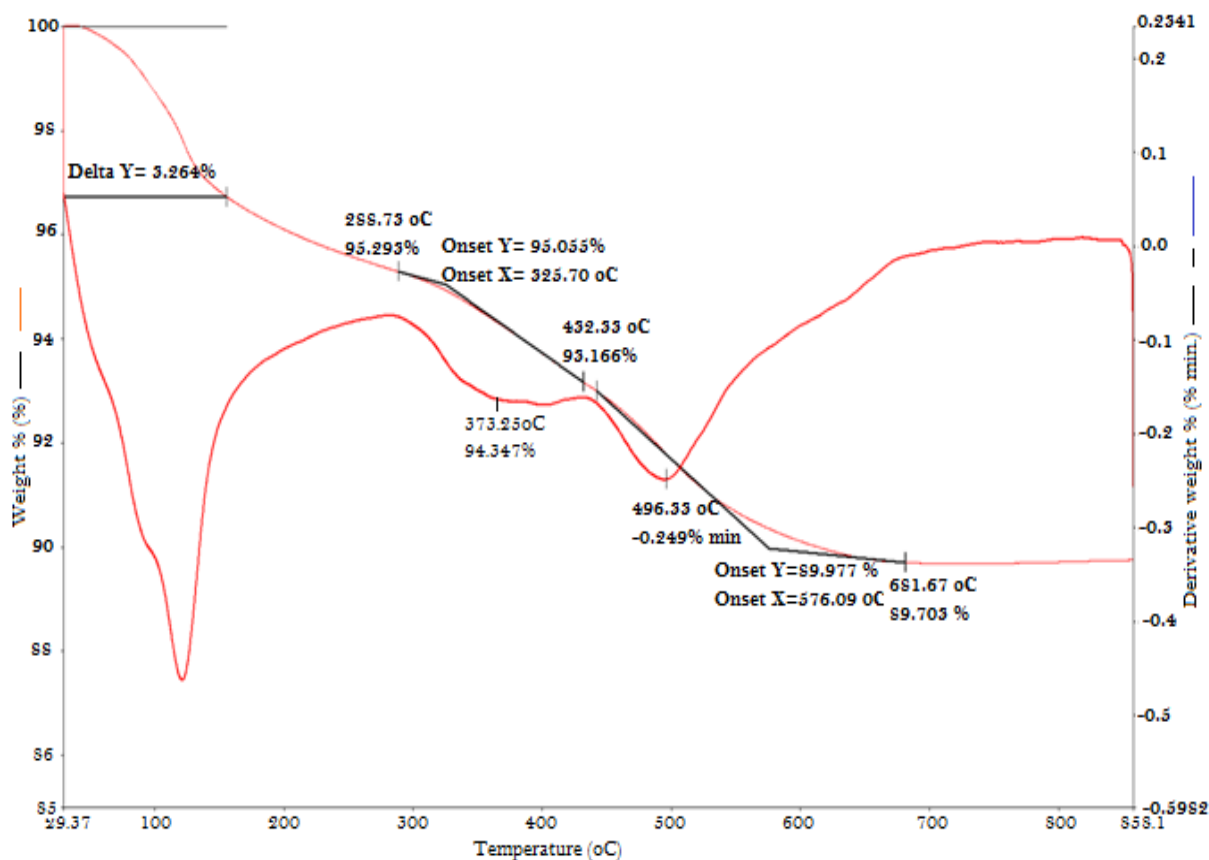


**Figure 7:** Thermogravimetric and Derivative Thermogravimetric analysis of GPC M2 (Si/Al: 2.5)

**Table 5:** Thermo-Gravimetric Analysis (TGA) of GPC

Sample	Peak degradation temperature, $T_p$ (°C)	$T_{5\%}$ (°C)	Onset temperature (°C)	Degradation temperature range (°C)	Moisture content (%)
GPC M1	413.00	365.49	355.68	305.70-439.14	3.48
	492.62		577.36	439.14-685.25	
GPC M2	373.25	318.13	325.70	288.70-432.33	3.26
	496.33		576.09	432.33-681.67	

Thermo-gravimetric analysis was performed on the GPC specimens to compare their thermal behavior after curing for 90 days at ambient conditions.

The weight loss of GPC M1 started at approximately 30°C with maximum weight loss temperature at approximately 98.9°C and was completed at approximately 300°C. This loss of weight can be attributed to the removal of water molecules absorbed (up to approximately 100°C) or differently linked (up to approximately 200°C, free water in the pores of the concrete; at higher temperatures, structural water and bound water in the nanopores) to the silicate molecules (Duxson *et al.*, 2007; Rosas *et al.*, 2014). The overall weight loss was 3.478% and geopolymer material residue of 96.522% remained.

After the loss of water in the concrete sample, the TGA curve showed degradation of the composition at two points. The concrete specimen was thermally stable up to about 300°C. At 305.70°C, the first degradation started which ended at 439.14°C, resulting in a weight loss of 2.728%. The second degradation process started at the temperature at which the first degradation stopped and was completed at 685.25°C recording a weight loss of about 3.571%. The two degradation steps can be attributed to the combustion of the dispersed organic phase. There was a total weight loss of 9.777%, leaving combustion residue of 90.222% at 800°C. The temperature at which 5% of the concrete sample would have degraded ( $T_5$ ) was 365.49°C.

The GPC M2 losses its water molecules at the temperature range of 30-150°C with maximum weight loss temperature of approximately 126.35°C and weight loss of about 3.264%. Two degradation points were also identified on the TGA/DTG curve (Figure 7), the first starting at 288.73°C and stopped at 432.33°C losing about 3.57% of its weight. The second degradation process started at 432.33°C and ended at 681.67°C with a weight loss of about 3.463%. The overall weight loss is 10.297% and the geopolymer material residue of 89.703% remained at 800°C. At 318.13°C, 5% of the concrete degraded.

The Thermo-Gravimetric Analysis revealed that both GPC M1 and M2 are thermally stable up to 300°C and the thermal treatment up to 800°C resulted in a complete removal of the organic phase from the composition.

### 3.2.4 Scanning Electron Microscopy (SEM) of Geopolymer Concrete

Scanning Electron micrographs of the GPCs studied exhibit significant change in the microstructure with variation of Si/Al ratio. In all the cases, (figure 8 A, B, C and D) there is evidence of strict adhesion between the components of the GPCs. The change in the microstructure appears more between the impact fractured surfaces of GPC M1 (Figure 8B) and GPC M2 (Figure 8D).

SEM of GPC M1 (figure 8B) identified components of the concrete such as the granite and portions of un-dissolved MK and aggregate. The surfaces of the aggregate upon impact were cleaner in this composition which revealed that there was no proper bonding between the aggregate and the MK matrix. The SEM image also showed a scarcely compact and porous structure. This could be due to the incomplete dissolution of the MK powder by the alkaline activating solution as identified by the X-Ray Diffractograms, thereby forming a weaker bond (Si-O-Al) between the geopolymer binder paste and the aggregate (fine and coarse).

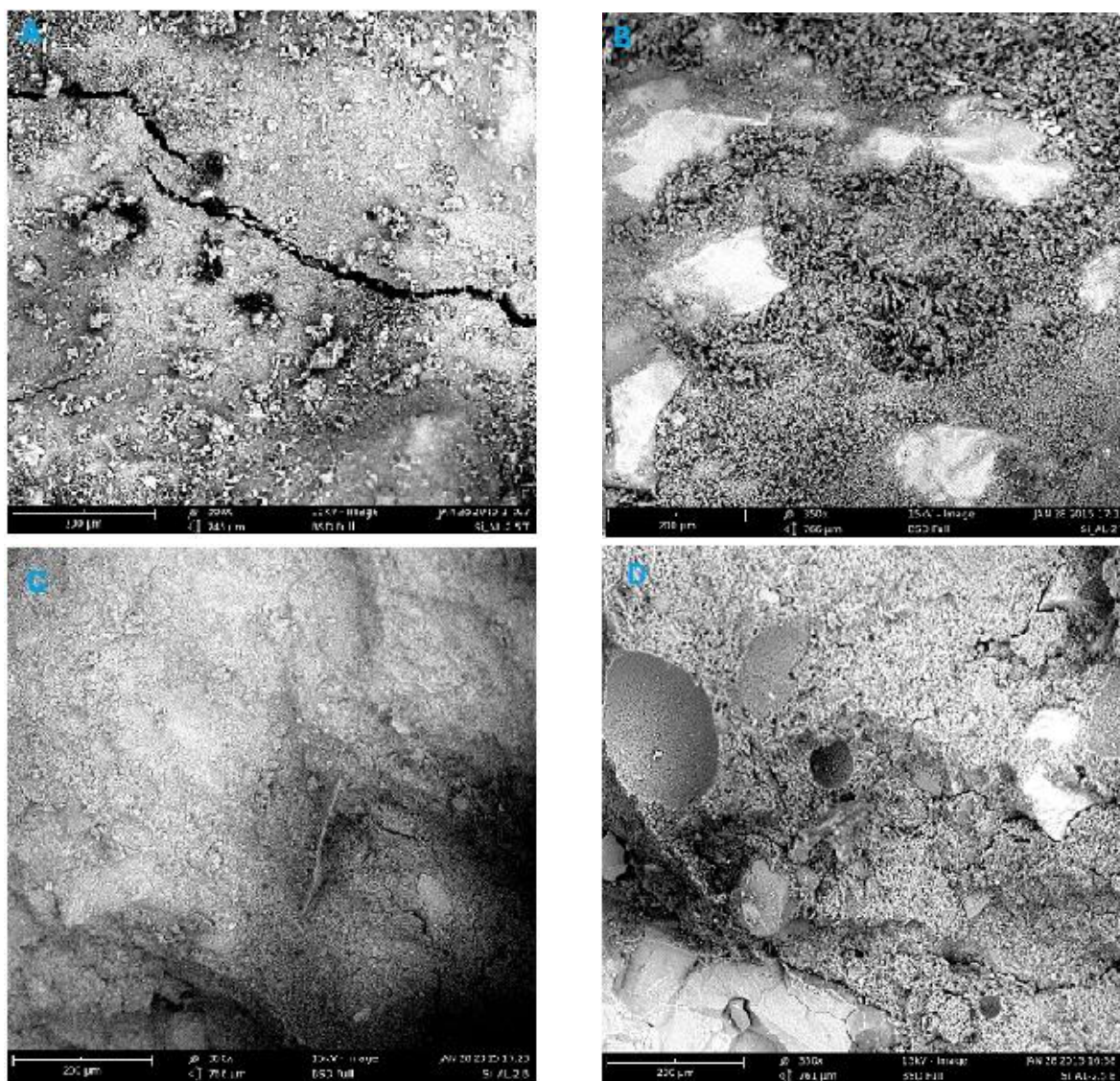


**Figure 8: (A, B, C and D):** Morphological features of GPC M1 (A and B) and GPC M2 (C and D) at 90- days curing.

The SEM image of GPC M2 (figure 8D) shows a better interaction between the aggregate and the MK matrix as the aggregate were seen to be well embedded within the matrix and portions of the matrix were still attached to the aggregate upon impact fracture. This revealed that the composition with Si/Al ratio 2.5 (GPC M2) resulted in the development of stronger bond between the components of the concrete. As was observed in the X-Ray diffraction patterns of the GPCs, there was a proper dissolution of the MK powder which interacted well with the aggregate to produce a homogenous hybrid material, thus, contributing to the increase in the

mechanical strength of the GPC. Such observation agrees well the conclusion that the higher the Si/Al ratio, the higher the degree of dissolution; and the higher the degree of reaction, the higher the compressive strength of the GPC (Alvarez-Ayuso et al., 2008).

### 3.4 Strength Properties of Geopolymer Concrete

Results of the strength properties (compressive and tensile) conducted on the GPCs are presented in Figures 9 and 10.

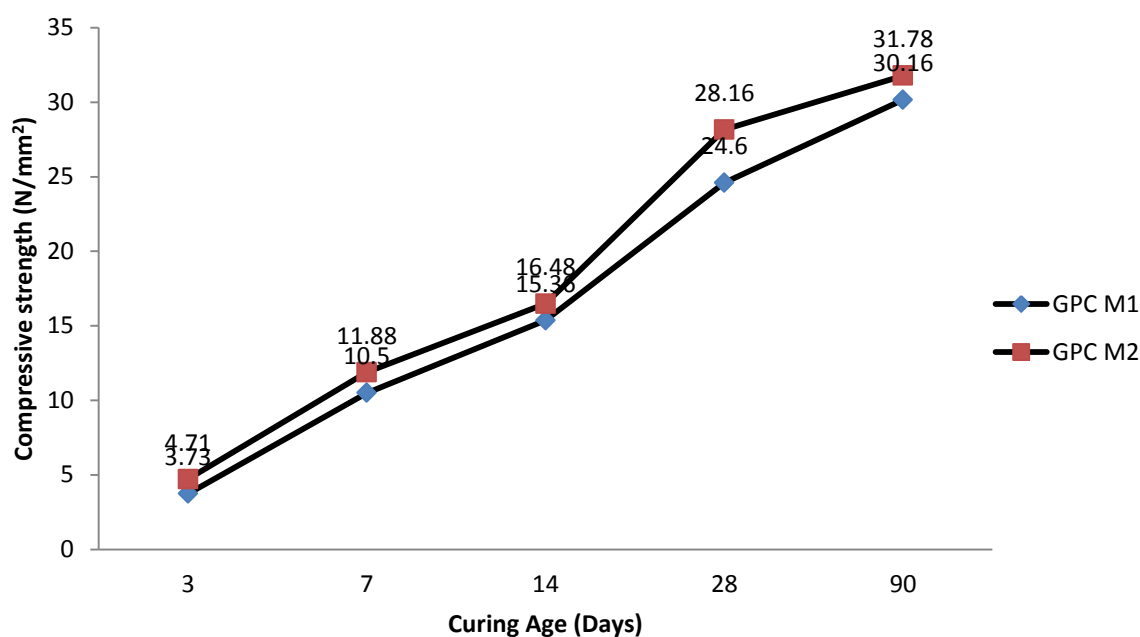


Figure 9: Compressive strength of GPC

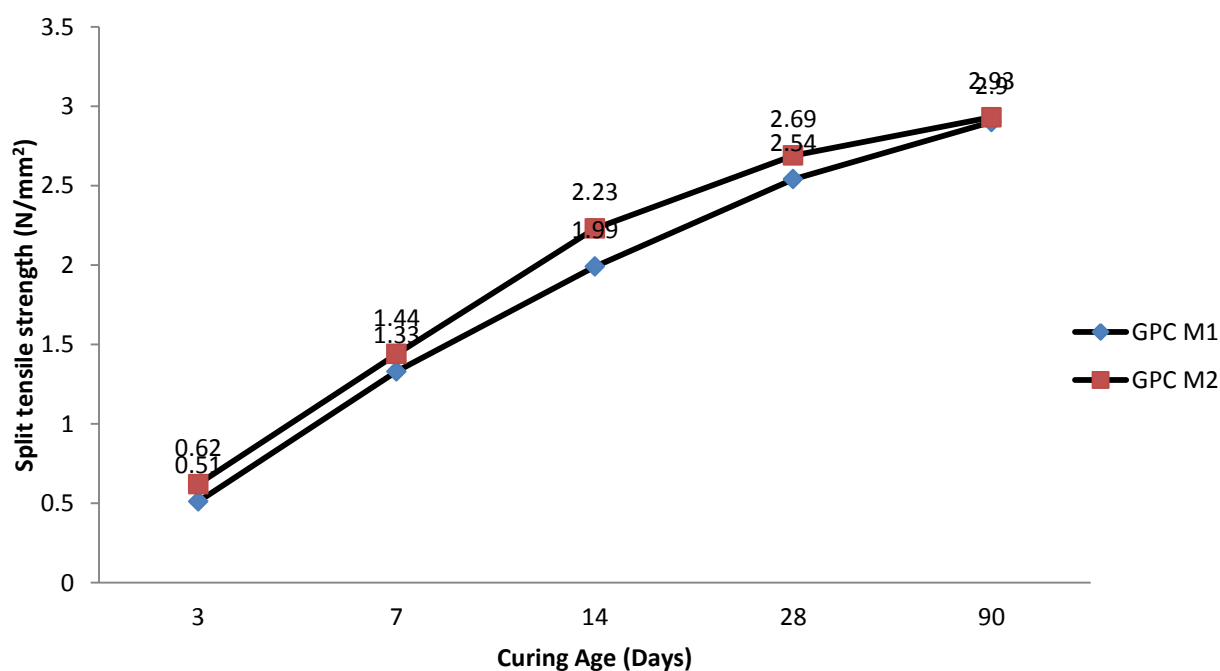


Figure 10: Split tensile strength of Geopolymer concrete

### **3.3.1 Compressive Strength of Geopolymer Concrete**

#### **3.3.1.1 Effect of Curing Age**

Figure 9 represents the compressive strength of GPC M1 and GPC M2. The compressive strength of 3.73 N/mm<sup>2</sup> and 4.71 N/mm<sup>2</sup> were recorded at 3 days by the GPC M1 and M2. The strength of GPC M1 appreciated to 10.50 N/mm<sup>2</sup> at 7 days indicating 181.5% increase on the strength at 3 days. On the other hand, GPC M2 attained a strength of 11.88 N/mm<sup>2</sup> representing 152.2% increase. The prompt strength gain at 7 days could be as a result of the shift of the Si-O vibration bands to lower wave numbers which confirmed geopolymerization reaction by the FTIR. Physical observation found that the GPC samples have expelled most of its water of hydration making it appear more drier than when observed at 3 days. This could also result to the rapid strength development at this age.

As the curing duration increased, a proportionate improvement in the compressive strength was also observed. At 14 days curing age, the compressive strength reached 15.36 N/mm<sup>2</sup> and 16.48 N/mm<sup>2</sup> representing 46.3% and 38.7% increase in strength for both GPCs M1 and M2 respectively.

After the 28-day curing the compressive strength was characterized by further increase of 60.1% for GPC M1 and 70.9% for GPC M2. The compressive strengths of the GPC at 28 days curing age falls under grade C20/25 which is considered as normal strength concrete in accordance with the specification of BS EN 206-1 2000 (concrete, specification and performance). The code states that the compressive strength of concrete is denoted by concrete strength classes, which relate to the characteristic cube strength ( $f_{ck}$ ) determined at 28 days. It is taken that at 28 days 75-85% of the strength of concrete has been attained.

At 90 days, the increase in strength of both GPC M1 and M2 was not significant. The maximum strength of 30.16 N/mm<sup>2</sup> was attained for M1 (Si/Al: 2.0) and 31.78 N/mm<sup>2</sup> for GPC M2 (Si/Al: 2.5) representing 22.6% and 12.9% increase in strength respectively. The increase in the compressive strength of the specimens at longer curing age suggests that the transient nature of geopolymerization extends into longer period and that the development is dependent on the Si/Al ratio (Mousa, 2013).

#### **3.3.1.2 Effect of Silicon/Aluminium Ratio**

GPC M2 was observed to have attained higher compressive strength than GPC M1 at all the curing ages considered. At 3 days the compressive strength of GPC M2 (Si/Al: 2.5) increased by 26.3% from the GPC M1 (Si/Al: 2.0). At 7, 14, 28- and 90-days curing ages, the GPCs M2 were characterized by 13.1%, 7.3%, 14.5% and 5.4% increase in the compressive strength respectively from the GPC M1. The formation of Si-O-Si-O-Al bond at the expense of Si-O-Al bonds confirmed by the FTIR and the higher rate of dissolution of the MK by the alkali activating solution at higher ratio as indicated by the XRD might have improve the compressive strength of GPC M2. This indicates that at higher Si/Al ratio, the strength properties of geopolymers increases, in so doing, making the structure more stable (Kim 2012).

### 3.3.2 Split Tensile Strength of Geopolymer Concrete

#### 3.3.2.1 Effect of Curing Age

Figure 10 represents the tensile strength of GPC M1 and M2. As in the case of the compressive strength, at 3-days curing age the split tensile strength of both GPC M1 and M2 ( $0.51 \text{ N/mm}^2$  and  $0.62 \text{ N/mm}^2$  respectively), were relatively low owing to the presence of water in the concrete samples. Appreciable split tensile strength development started at the 7-days in which the GPC M1 reached strength of  $1.33 \text{ N/mm}^2$  equivalent to 160.8% increase in the split tensile strength from the 3 days curing age. At that same age, the GPC M2 attained strength of  $1.44 \text{ N/mm}^2$  representing 134.3% increase.

It was evident that there was a gradual appreciation of strength for both GPC M1 and GPC M2 at 14, 28 and 90 days curing age representing 49.6%, 28.1% and 13.7% increase in split tensile strength for GPC M1 respectively and 54.9%, 20.6% and 11.4% increase for GPC M2.

#### 3.3.2.2 Effect of Silicon/Aluminium Ratio

The result of the split tensile test of the GPC M2 showed higher split tensile strength than that of GPC M1. At curing age of 3, 7, 14, 28 and 90 days the split tensile strength of GPC M2 was represented by 21.6%, 8.3%, 12.0%, 5.5% and 1.0% increase in split tensile strength from GPC M1 respectively. It can therefore be concluded that the Si/Al ratio has a significant effect on the split tensile strength of GPC. The increase in Si/Al ratio is directly proportional to the increase in the split tensile strength.

## 4.0 Conclusion

The FTIR analysis showed that geopolymerization has occurred by the disappearance of the Si-O-Al vibration band at  $775 \text{ cm}^{-1}$  in all the samples of the GPC. The shift of the characteristic band at  $1028 \text{ cm}^{-1}$  relating to the Si-O asymmetric stretching towards lower wave numbers which indicates the formation of new structure different from the MK also confirms geopolymerization. Increase in the Si/Al ratio led to the displacement of Al by Si thereby forming more Si-O-Si-O-Al bonds resulting to the increase in the mechanical strength of the GPC M2 as confirmed by the XRD and the compressive strength test.

The XRD revealed that both the GPC M1 and M2 are amorphous in nature and as the Si/Al ratio increased, there was higher rate of dissolution of the MK by the alkaline activating solution and improvement in the stability of the structure, as supported by the SEM images of the geopolymer specimens.

The GPC is thermally stable up to  $300^\circ\text{C}$  as detected by the TGA and can withstand temperature of  $800^\circ\text{C}$  as only the organic phases in the concrete degraded at that temperature.

The SEM of the GPC M1 showed a scarcely compact and porous structure due to the incomplete dissolution of the MK at that ratio. But the SEM of GPC M2 revealed a firm adhesion with stronger interaction between the components of the concrete.

The GPC synthesized from Alkaliner kaolin at ambient temperature exhibited good mechanical properties (compressive and split tensile strengths) acceptable for use as normal strength concrete (concrete grade C20/25 as specified in the requirement of BS EN 206-1 2000). The strengths improved with increase in the Si/Al ratio and the curing ages of the concrete.

The study recommends that with the limited understanding of the microstructural behavior and thermal properties of the GPC more experiments such as the Magic Angle Spinning-Nuclear Magnetic Resonance (MAS-NMR), Energy-dispersive X-ray Spectroscopy (EDXS) and Differential Scanning Calorimetry (DSC) should be carried out to provide better comprehension on the nature of the material in order that it may find different applications within the Nigerian construction industry.

## References

- Al-Shathr, B., Al-Attar, T. and Hasan, Z. 2016. Effect of curing system on metakaolin based geopolymer concrete. *Journal of Babylon University: Engineering Sciences*, 24(3): 569-576.
- Alvarez-Ayuso, E., Querol, X., Plana, F., Alastuey, A., Moreno, N., Izquierdo, M., ... Barra, M. 2008. Environmental, Physical and Structural Characterisation of Geopolymer Matrixes Synthesised from Coal (Co-) Combustion Fly Ashes. *Journal of Hazardous Materials*, 154: 175-183.
- Andrew, RM. 2018. Global CO<sub>2</sub> Emissions from Cement Production. *Earth System Science Data*. 10: 195-217.
- Barbosa, VFF., Mackenzie, KJD. and Thaumaturgo, C. 2000. Synthesis and characterization of materials based on inorganic polymers of alumina and silica: Sodium polysialate polymers. *International Journal of Inorganic Materials*, 2 (4): 309-317.
- Bashir, I., Kapoor, K. and Sood, H. 2017. An Experimental Investigation on the Mechanical Properties of Geopolymer Concrete. *International Journal of Latest Research in Science and Technology*, 6(3): 33-36.
- British Geological Survey: Mineral Profile 2005. Cement Raw Materials. Natural Environmental Research Council, Office of the Deputy Prime Minister.
- Claudio, F., Francesco, C., Giuseppina, R., Domenico, A., Costantino, M., Alberto, B., ... Gaetano, M. 2013. Application-Oriented chemical optimization of a metakaolin Based geopolymer. *Journal of Materials*, 6 (5): 1920-1939.
- Das, SK., Mishra, J. and Mustakim, SM. 2018. An Overview of Current Research Trends in Geopolymer Concrete. *International Research Journal of Engineering and Technology (IRJET)* 05(11): 376-381.
- Diaz-Loya, IE., Allouche, EN., and Vaidya, S. 2011. Mechanical Properties of Fly-Ash Based Geopolymer Concrete. *ACI Materials Journal*, 108(3): 300-306.
- Duxson, P., Lukey, GC., Mallicoat, SW., Kriven, WM. And Van Deventer, JSJ. 2007. Effect of alkali and Si/Al ratio on the development of mechanical properties of metakaolin-based geopolymers. *Colloids and Surfaces A: Physicochemical Engineering Aspects*, 292 (1): 8-20.

Fernandez-Jimenez, AM., Palomo, A. and Lopez-Hombrados, C. 2006. Engineering Properties of Alkali Activated Fly-Ash Concrete. *ACI Materials Journal*, 103(2): 106-112.

Guo, X., Shi, H. and Dick, WA. 2010. Compressive strength and microstructural characterization of class C fly ash geopolymer. *Cement and Concrete composites*, 32 (2): 142-147.

He, J., Zhang, J., Yu, Y., and Zhang, G. 2011. The Strength and Microstructure of Two Geopolymers Derived Metakaolin and Red mud and Fly Ash Mixture: A Comparative Study. *Construction and Building Materials*, 30 (1): 80-91.

Kamarudin, H., Mustafa, A., Abdullah, MMA., Binhussain, M., Ruzaidi, C., Musa, L., Yong, H. and Ming, L. 2011. Preliminary Study on Effect of NaOH Concentration on Early Age Compressive Strength of Kaolin-Based Green Cement. *International Conference on Chemistry and Chemical Process IPCBEE*. 10.

Khale, D. and Chaudhary, R. 2007. Mechanism of geopolymerization and factors influencing its development: A review. *Journal of Material Science*, 42 (3): 729-746.

Kim, EH. 2012. Understanding the Effects of Silicon/Aluminium ratio and calcium hydroxide on the chemical composition, nanostructure and compressive strength for metakaolin geopolymers. Master's thesis submitted to the Department of Civil Engineering, University of Illinois.

Kong, DLY., Sanjayan, JG. and Sagoe-Crentsil, K. 2007. Comparative performance of geopolymers made with metakaolin and fly ash after exposure to elevated temperatures. *Cement and concrete research*, 37 (12): 1583-1589.

Lateef NA, Edward, D., Mohamed, KE. and Paul, Z. 2016. Investigation of early compressive strength of fly Ash-Based Geopolymer Concrete. *Construction and Building Materials*. 112(1): 807-815.

Liang, C., Zaiqin, W., Yuanyi, W. and Jing, F. 2016. Preparation and Properties of Alkali Activated Metakaolin-Based Geopolymer. *Materials*, 9(767): 1-12.

Malewar, Y., Saleem, S. and Titiksh, A. 2017. Gap Grading of Aggregates and Its Effect on The Inherent Properties of Concrete. *MAT Journal of Ceramics and Concrete Sciences*. 2: 1-8.

Mousa, G. 2013. Geopolymers from Jordanian Metakaolin: Influence of Chemical and Mineralogical Compositions on the Development of Mechanical Properties. *Jordan Journal of Civil Engineering*, 7(2): 606-629.

Najet, S., Basma, S. and Samir, B. 2013. Effect of composition on structure and mechanical properties of Metakaolin based PSS-Geopolymer. *International Journal of Materials Science (IJMSCI)*, 3 (4): 145-151.

Nasab GM., Golestanifard F. and MacKenzie KJD. 2014. The Effect of the SiO<sub>2</sub>/Na<sub>2</sub>O ratio in the structural modification of metakaolin-based geopolymers studied by XRD, FTIR and MAS-NMR. *Journal of Ceramic Science and Technology*, 5(3): 185-192.

Naqi, A. and Jang, GJ. 2019. Recent Progress in Green Cement Technology Utilizing Low-Carbon Emission Fuel and Raw material. A Review. *Journal of Sustainability* 11(537): 1-18. doi:10.3390/su11020537

Neupane, K., Chalmers, D. and Kidd, P. 2018. High-Strength Geopolymer Concrete- Properties, Advantages and Challenges. *Advances in Materials*, 7(2); 15-25. doi:10.11648/j.am.20180702.11.

Neville, A. M. (2000). *Properties of Concrete*, Prentice Hall.

Pawar, C., Sharma, P. and Titiksh, A. 2016. Gradation of Aggregates and its Effects on Properties of Concrete. *International Journal of Trend in Research and Development*. 3: 2394-9333.

Rattanasak, U. and Chindaprasirt, P. 2009. Influence of NaOH solution on the synthesis of fly ash geopolymer. *Minerals Engineering*, 22 (12): 1073-1078.

Rosas, C., Arredondo-Rea, S., Gómez-Soberón, J., Almaral, J., Corral Higuera, R., Chinchillas-Chinchillas, MJ. and Acuña-Agüero, O. 2014. Experimental study of XRD, FTIR and TGA techniques in geopolymeric materials. *International Journal for Housing Science and Its Applications*, 4(4): 221-227.

Rovnanik, P. 2010. Effect of Curing Temperature on the Development of Hard Structure of Metakaolin-based Geopolymer. *Construction and Building Materials*, 24(7); 1176-1183.

Shabarish, P., Veeresh, BK. and Manojkumar, C. 2018. Granulated Blast-Furnace Slag (GGBS) based Geopolymer Concrete- Review Concrete- Review. *International Journal of Advanced Science and Engineering*. 5(1): 879-885. Doi:10.29294/IJASE.5.1.2018.789-885.

Soleimani, MA., Naghizadeh, R., Mirhabibi, AR. and Golestanifard, F. 2012. Effect of calcination temperature of the kaolin and molar  $\text{Na}_2\text{O}/\text{SiO}_2$  activator ratio and physical and microstructural properties of metakaolin based geopolymers. *Iranian Journal of Material Science and Engineering*, 9 (4): 43-51.

Thapa, VB. and Waldmann, D. 2018. A short review on alkali-activated binders and geopolymer binders.

Usman, ND., Salihu, CH., Solomon, MS., Abeku DM., and Isa, FN. 2020. Influence of Silicon/Aluminium ratio on the Strength Properties of Kaolin (Metakaolin) Geopolymer Mortar in Alkaleri, Bauchi state Nigeria. *Journal of Building and Environmental Engineering* 1(1): 23-33.

Xu, H. and Van Deventer, JSJ. 2000. The geopolymerization of aluminosilicate minerals. *International journal of Mineral Processing*, 59 (3): 247-266.

Zhang, YS., Sun, W. and Zongjin, L. 2010. Composition Design and Microstructural Characterization of Calcined Kaolin-Based Geopolymer Cement. *Applied Clay Science*, 47 (3): 271-275.

ASTM C. 2003 39/C39M-03. Standard Test Method for Compressive Strength of Cylindrical Concrete Specimens. *Journal of American Society for Testing and Materials*. 5 (10).

ASTM C. 2017 496/C496-17. Standard Test Method for Splitting Tensile Strength of Cylindrical Concrete Specimens. ASTM International, West Conshohocken, PA, Retrieved from: [www.astm.org](http://www.astm.org).

ASTM C. 2010 128-07a. Standard Test Method for Density, Relative Density (Specific gravity), and Absorption of Fine Aggregate.

BS EN 206-1 2000. Concrete – Part 1: Specification, performance, production and conformity. European Committee for Standardization, 20-21